



# The Platelet Lipidome Is Altered in Patients with COVID-19 and Correlates with Platelet Reactivity

Alex R. Schuurman<sup>1,\*</sup> Valentine Léopold<sup>1,2,\*</sup> Liza Pereverzeva<sup>1</sup> Osoul Chouchane<sup>1</sup>  
Tom D. Y. Reijnders<sup>1</sup> Justin de Brabander<sup>1</sup> Renée A. Douma<sup>3</sup> Michel van Weeghel<sup>4,5</sup> Eric Wever<sup>4,5,6</sup>  
Bauke V. Schomaker<sup>4,5</sup> Frédéric M. Vaz<sup>4,5,7</sup> Willem Joost Wiersinga<sup>1,8</sup> Cornelis van't Veer<sup>1</sup>  
Tom van der Poll<sup>1,8</sup>

<sup>1</sup>Center for Experimental and Molecular Medicine (CEMM), Amsterdam University Medical Centers - Location AMC, University of Amsterdam, Amsterdam, The Netherlands

<sup>2</sup>Department of Anesthesia and Intensive Care, Hôpital Lariboisière, INSERM U942S MASCOT, Université de Paris, Paris, France

<sup>3</sup>Department of Internal Medicine, Flevo Hospital, Almere, The Netherlands

<sup>4</sup>Departments of Clinical Chemistry and Pediatrics, Laboratory Genetic Metabolic Diseases, Amsterdam Gastroenterology Endocrinology Metabolism, Amsterdam UMC, University of Amsterdam, Amsterdam, The Netherlands

<sup>5</sup>Department of Epidemiology & Data Science, Bioinformatics Laboratory, Amsterdam Public Health Research Institute, Amsterdam UMC, University of Amsterdam, Amsterdam, The Netherlands

Address for correspondence Valentine Léopold, MD, MSc, Amsterdam UMC, University of Amsterdam, Centre for Experimental and Molecular Medicine, Meibergdreef 9, 1105 AZ, Amsterdam, The Netherlands (e-mail: v.leopold@amsterdamumc.nl).

<sup>6</sup>Core Facility Metabolomics, Amsterdam UMC, Amsterdam, The Netherlands

<sup>7</sup>Department of Pediatrics, Emma Children's Hospital, Amsterdam UMC, University of Amsterdam, Amsterdam, The Netherlands

<sup>8</sup>Division of Infectious Diseases, Amsterdam University Medical Centers - Location AMC, University of Amsterdam, Amsterdam, The Netherlands

Thromb Haemost 2022;122:1683–1692.

## Abstract

**Background** Activated platelets have been implicated in the proinflammatory and prothrombotic phenotype of coronavirus disease 2019 (COVID-19). While it is increasingly recognized that lipids have important structural and signaling roles in platelets, the lipidomic landscape of platelets during infection has remained unexplored.

**Objective** To investigate the platelet lipidome of patients hospitalized for COVID-19.

**Methods** We performed untargeted lipidomics in platelets of 25 patients hospitalized for COVID-19 and 23 noninfectious controls with similar age and sex characteristics, and with comparable comorbidities.

**Results** Twenty-five percent of the 1,650 annotated lipids were significantly different between the groups. The significantly altered part of the platelet lipidome mostly comprised lipids that were less abundant in patients with COVID-19 (20.4% down, 4.6% up, 75% unchanged). Platelets from COVID-19 patients showed decreased levels of membrane plasmalogens, and a distinct decrease of long-chain, unsaturated triacylglycerols. Conversely, platelets from patients with COVID-19 displayed class-wide

## Keywords

- ▶ platelets
- ▶ platelet activation
- ▶ lipidomics
- ▶ COVID-19
- ▶ plasmalogens

\* A.R.S. and V.L. are co-first authors.

received

December 9, 2021

accepted after revision

March 30, 2022

published online

July 18, 2022

DOI <https://doi.org/>

10.1055/s-0042-1749438.

ISSN 0340-6245.

© 2022. The Author(s).

This is an open access article published by Thieme under the terms of the Creative Commons Attribution-NonDerivative-NonCommercial-License, permitting copying and reproduction so long as the original work is given appropriate credit. Contents may not be used for commercial purposes, or adapted, remixed, transformed or built upon. (<https://creativecommons.org/licenses/by-nc-nd/4.0/>)

Georg Thieme Verlag KG, Rüdigerstraße 14, 70469 Stuttgart, Germany

higher abundances of bis(monoacylglycerol)phosphate and its biosynthetic precursor lysophosphatidylglycerol. Levels of these classes positively correlated with ex vivo platelet reactivity—as measured by P-selectin expression after PAR1 activation—irrespective of disease state.

**Conclusion** Taken together, this investigation provides the first exploration of the profound impact of infection on the human platelet lipidome, and reveals associations between the lipid composition of platelets and their reactivity. These results warrant further lipidomic research in other infections and disease states involving platelet pathophysiology.

## Introduction

The role of platelets in coronavirus disease 2019 (COVID-19) has been under the spotlight due to the high occurrence rate of thromboembolic events throughout the disease course.<sup>1–3</sup> Whether platelets are directly targeted by severe acute respiratory syndrome coronavirus 2 (SARS-CoV-2), the causative agent in COVID-19, remains controversial, and there are contradictory reports regarding the presence of SARS-CoV-2 RNA in platelets.<sup>4–7</sup> However, it is well established that circulating platelets are activated in COVID-19 patients: they display a procoagulant and proinflammatory phenotype which contributes to the reported prothrombotic state of the disease.<sup>8–10</sup>

Lipids have essential structural and signaling roles in platelets, and lipidome remodeling is important in platelet activation and functionality.<sup>11</sup> For instance, cell membrane fluidity—dictated by phospholipid scrambling and abundance of cholesterol and sphingolipids—influences degranulation and cell–cell adhesion.<sup>12</sup> Lipid rafts, dynamic nanosized platforms consisting of lipids and proteins, mediate signal transduction, extracellular-vesicle release, and platelet aggregation.<sup>13</sup> The involvement of the platelet lipidome during activation was highlighted in a recent study, showing that up to 20% of the lipidomic profile of platelets was changed upon ex vivo stimulation.<sup>14</sup> Furthermore, it was recently shown that the platelet lipidome differed between patients with acute and chronic coronary syndrome, and that upregulation of specific glycerophospholipids increased platelet activation and thrombus formation.<sup>15</sup> To our knowledge, analysis of the human platelet lipidome during infection has not yet been reported. Such an approach could be highly informative of integral changes underlying platelet functionality and pathophysiology during infection.

To this end, we performed untargeted lipidomic analysis of platelets isolated from hospitalized patients with COVID-19 and comparable noninfectious control subjects. We comprehensively describe the profound impact of infection on the platelet lipidome, and correlate specific lipid classes to platelet reactivity.

## Methods

### Inclusion of Patients and Isolation of Platelets

Patients were included in the ELDER-BIOME cohort (clinicaltrials.gov identifier NCT02928367).<sup>16</sup> We prospectively enrolled suspected COVID-19 patients admitted to the ward,

in two hospitals in the Netherlands (Amsterdam University Medical Centers [UMC] in Amsterdam and the Flevo Hospital in Almere). SARS-CoV-2 infection was confirmed by polymerase chain reaction (PCR) of material obtained by nasopharyngeal swab. Patients were included within 48 hours after hospital admission. Controls were hospital employees ( $n=8$ ) or patients visiting the outpatient clinic without infectious disease symptoms ( $n=15$ ). Written informed consent was obtained from patients and controls prior to blood draw and according to the local ethics committee recommendations (Medisch Ethische Toetsings Commissie—METC protocol number NL57847.018.16). Citrated blood was collected by peripheral venous puncture and kept at room temperature during routing to Amsterdam UMC. Controls were punctured at the same time as COVID-19 patients, and every COVID-19 sample was processed in parallel to a control sample within 4 hours after withdrawal. Platelet-rich plasma was obtained by centrifugation (180 g, 15 minutes, 21°C), mixed with a 1:5 ratio of acid citrate dextrose, and subsequently centrifuged (200 g, 2 minutes) to remove remaining erythrocytes and leukocytes. Platelet number was established by flow cytometry, using Precision Count Beads (BD Bioscience, San Jose, California, United States). A total of 125 million platelets were then spun (800 g, 10 minutes, 21°C), washed with phosphate-buffered saline containing EDTA 0.35 mM, bovine serum albumin 0.1%, and the pellet was snap-frozen in liquid nitrogen and kept at –80°C until analysis. This isolation protocol was optimized and validated experimentally using samples from healthy subjects by flow cytometry. Platelet pellets had a high purity (99.6% [99.2–99.8]) and low activation status (2–5% CD62P+, 4–10% CD63+, and 2% active GpIIb/IIIa positive platelets). Some of the patients and controls in this study were part of a previous study published by our group.<sup>8</sup>

### Lipidomics

Lipidomics analysis was performed as previously described, with minor adjustments.<sup>17</sup> In a 2 mL tube, the following amounts of internal standards dissolved in 1:1 (v/v) methanol:chloroform were added to each sample: bis(monoacylglycerol)phosphate BMP(14:0)<sub>2</sub> (0.2 nmol), ceramide-1-phosphate C1P(d18:1/12:0) (0.125 nmol), D<sub>7</sub>-cholesteryl ester CE(16:0) (2.5 nmol), ceramide Cer(d18:1/12:0) (0.125 nmol), ceramide Cer(d18:1/25:0) (0.125 nmol), cardiolipin CL(14:0)<sub>4</sub> (0.1 nmol), diacylglycerol DAG(14:0)<sub>2</sub> (0.5 nmol),

glucose ceramide GlcCer(d18:1/12:0) (0.125 nmol), lactose ceramide LacCer(d18:1/12:0) (0.125 nmol), lysophosphatidic acid LPA(14:0) (0.1 nmol), lysophosphatidylcholine LPC(14:0) (0.5 nmol), lysophosphatidylethanolamine LPE(14:0) (0.1 nmol), lysophosphatidylglycerol LPG(14:0) (0.02 nmol), phosphatidic acid PA(14:0)<sub>2</sub> (0.5 nmol), phosphatidylcholine PC(14:0)<sub>2</sub> (2 nmol), phosphatidylethanolamine PE(14:0)<sub>2</sub> (0.5 nmol), phosphatidylglycerol PG(14:0)<sub>2</sub> (0.1 nmol), phosphatidylinositol PI(8:0)<sub>2</sub> (0.5 nmol), phosphatidylserine PS(14:0)<sub>2</sub> (5 nmol), sphinganine-1-phosphate S1P(d17:0) (0.125 nmol), sphinganine-1-phosphate S1P(d17:1) (0.125 nmol), ceramide phosphocholines SM(d18:1/12:0) (2.125 nmol), sphingosine SPH(d17:0) (0.125 nmol), sphingosine SPH(d17:1) (0.125 nmol), triacylglycerol TAG(14:0)<sub>2</sub> (0.5 nmol). All internal standards were purchased from Avanti Polar Lipids, Alabaster, Alabama, United States. 1.5 mL 1:1 (v/v) methanol:chloroform was added before thorough mixing. The samples were then centrifuged for 10 minutes at 14,000 rpm, supernatant transferred to a glass vial, and evaporated under a stream of nitrogen at 60°C. The residue was dissolved in 150 µL of 1:1 (v/v) methanol:chloroform. Lipids were analyzed using a Thermo Scientific Ultimate 3000 binary HPLC coupled to a Q Exactive Plus Orbitrap mass spectrometer. For normal phase separation, 5 µL of each sample was injected onto a Phenomenex LUNA silica, 250 × 2 mm, 5 µm 100 Å. Column temperature was held at 25°C. Mobile phase consisted of (A) 85:15 (v/v) methanol:water containing 0.0125% formic acid and 3.35 mmol/L ammonia and (B) 97:3 (v/v) chloroform:methanol containing 0.0125% formic acid. Using a flow rate of 0.3 mL/min, the liquid chromatography (LC) gradient consisted of: dwell at 10% A 0 to 1 minute, ramp to 20% A at 4 minutes, ramp to 85% A at 12 minutes, ramp to 100% A at 12.1 minutes, dwell at 100% A 12.1 to 14 minutes, ramp to 10% A at 14.1 minutes, dwell at 10% A for 14.1 to 15 minutes. For reversed phase separation, 5 µL of each sample was injected onto a Waters HSS T3 column (150 × 2.1 mm, 1.8 µm particle size). Column temperature was held at 60°C. Mobile phase consisted of (A) 4:6 (v/v) methanol:water and (B) 1:9 (v/v) methanol:isopropanol, both containing 0.1% formic acid and 10 mmol/L ammonia. Using a flow rate of 0.4 mL/min, the LC gradient consisted of: dwell at 100% A at 0 minute, ramp to 80% A at 1 minute, ramp to 0% A at 16 minutes, dwell at 0% A for 16 to 20 minutes, ramp to 100% A at 20.1 minutes, dwell at 100% A for 20.1 to 21 minutes. MS data were acquired using negative and positive ionization by continuous scanning over the range of *m/z* 150 to *m/z* 2,000. Data were analyzed using an in-house developed lipidomics pipeline written in the R programming language (<http://www.r-project.org>). Lipid identification was based on a combination of accurate mass, (relative) retention times, fragmentation spectra (when required), analysis of samples with known metabolic defects, and the injection of relevant standards. Lipid classes are defined in our lipidomics pipeline in terms of their generic chemical formula, where R represents the radyl group. Upon import of the lipid database in the annotation pipeline the generic chemical formula of each lipid class is expanded by replacing the R-element with a range of possible radyl group

lengths and double-bond numbers. The resulting expanded list of chemical formulas is then used to calculate the neutral monoisotopic mass of each species. The expanded list is shown in ► **Supplementary Table S1** (available in the online version). This approach yielded data on 1,650 platelet lipids that were normalized on an extensive set of internal standards as listed above. The reported lipid abundances are semiquantitative and calculated by dividing the response of the analyte (area of the peak) by that of the corresponding internal standard multiplied by the concentration of that internal standard (arbitrary unit, A.U). The notation -o indicates lipids containing an alkyl-ether group, whereas -p indicates an alkenyl-ether group. When the nature of the ether species (alkyl/alkenyl) is unknown or cannot be chromatographically separated, this is indicated by the suffix o + p. As no dedicated internal standard for ether lipids are available, we used the PC(14:0)<sub>2</sub> and PE(14:0)<sub>2</sub> to normalize the corresponding ether lipid species (see ► **Supplementary Methods** and ► **Supplementary Fig. S1** [available in the online version] for details on the annotation). See ► **Supplementary Table S2** [available in the online version] for lipid class definitions.

### Flow Cytometry

Measurement of platelet activation and reactivity to protease activating receptor-1 (PAR1) stimulation was done as previously described.<sup>8</sup> Briefly, platelets in platelet-rich plasma were stimulated for 30 minutes with phosphate-buffered saline (control) or thrombin receptor activator peptide-6 (TRAP; Bachem, Bubendorf, Switzerland; 15 µM). Platelet activation was assessed by flow cytometry using FACS Canto-II and anti-CD61-Alexa Fluor 700 and anti-CD62P-PerCP-Cy5.5 (Biolegend, San Diego, California, United States). Data were analyzed using FlowJo v10 (BD Biosciences, San Jose, California, United States).

### Statistical Analysis

All statistical analyses were performed using R version 4.0.4. In the box and whisker plots, data are represented with a median line and a box indicating the interquartile range, with individual data points shown. Statistical significance of class-wide differences was determined using the two-sided Wilcoxon rank-sum test, with significance defined as *p* < 0.05. All species-specific analyses were corrected for multiple testing using the Benjamini–Hochberg method, with significance defined as an adjusted *p* < 0.05. Correlation analyses were performed using the R-package *corr*. Spearman's rho was calculated to quantify the strength of the correlation. All correlation analyses were corrected for multiple testing using the Benjamini–Hochberg method, with significance defined as an adjusted *p* < 0.05.

## Results

### Clinical Characteristics

We isolated and profiled resting platelets from 25 patients hospitalized for COVID-19 during the first “wave” of the pandemic in the Netherlands (April–May 2020) and 23 noninfected control subjects (controls), either hospital

workers or subjects visiting the outpatient clinic for a blood draw, without signs of acute infection (► **Table 1**). SARS-CoV-2 infection was confirmed at admission by PCR on a nasopharyngeal swab. The patient and control groups had similar age and sex characteristics. As we recruited noninfectious controls from the outpatient clinic, comorbidities and chronic medications were also largely similar between groups. Patients were not treated with therapeutic anticoagulation therapy or dexamethasone at admission, as this was not standard of care at the time of inclusion. Patients had a mean hospital length of stay of 6 days, a low number of intensive care admissions (2/25, 8%), and a 28-day mortality rate of 16% (4/25).

### The Platelet Lipidome Is Altered in Patients with COVID-19

We first investigated differences in the platelet lipidome of patients with COVID-19 and noninfectious controls using an untargeted approach. Principal component analysis (PCA), a dimensionality reduction method for visualizing data variance,<sup>18</sup> revealed a clear but partial separation between patients and controls (► **Fig. 1A**). To evaluate these differences on a lipid-specific level, we plotted the log<sub>2</sub> fold change and statistical significance of each lipid between groups in a volcano plot (► **Fig. 1B**) and ► **Supplementary Table S3** [available in the online version]. In line with the modest separation on the PCA, most lipids were not significantly different

**Table 1** Characteristics of patients and control subjects

	Controls (n = 23)	COVID-19 (n = 25)	p-Value
<b>Demographics</b>			
Age (y)	53.3 (18.8)	60.8 (13.0)	0.12
Gender (male), n (%)	11 (47.8)	12 (48.0)	>0.99
BMI	27.0 (7.5)	29.7 (4.8)	0.16
<b>Medical history</b>			
Hypertension (medicated), n (%)	8 (34.8)	9 (36.0)	>0.99
Prior stroke, n (%)	2 (8.7)	1 (4.0)	0.60
Diabetes mellitus, type 2, n (%)	5 (21.7)	5 (20.0)	>0.99
Atherosclerosis, n (%)	1 (4.3)	1 (4.0)	>0.99
Chronic kidney disease, n (%)	0 (0.0)	2 (8.0)	0.49
Prior malignancy, n (%)	4 (17.4)	1 (4.0)	0.18
<b>Chronic medication</b>			
Platelet aggregation inhibitors, n (%)	3 (13.0) <sup>a</sup>	2 (8.0) <sup>b</sup>	0.66
Statins, n (%)	5 (21.7)	4 (16.0)	0.49
<b>Disease course</b>			
qSOFA <sup>c</sup> (on admission)	–	1 [0.0, 1.0]	
MEWS <sup>d</sup> (on admission)	–	3 [2.0, 5.0]	
PSI <sup>e</sup> (on admission)	–	2 [1.0, 5.0]	
Mortality (day 28), n (%)	–	4 (16.0)	
Hospital length of stay (days)	–	6.2 (7.8)	
ICU admission, n (%)	–	2 (8.0)	
<b>Laboratory tests<sup>f</sup></b>			
Creactive protein (mg/L)	–	111.42 (69.13)	
Platelets ( $\times 10^9/L$ )	290 (166)	274 (108)	0.79
Leukocytes ( $\times 10^9/L$ )	5.8 [3.6–16.3]	6.9 [3.3–25.9]	0.22
Neutrophils ( $\times 10^9/L$ )	3.8 [1.5–10.2]	5.0 [1.5–21.2]	0.04
Lymphocytes ( $\times 10^9/L$ )	1.2 [0.8–3.4]	0.9 [0.2–3.3]	0.08

Note: Continuous data are presented as mean (standard deviation) or median [range], and compared using a two-sided one-way analysis of variance (equal variances not assumed) or two-sided Kruskal–Wallis test, respectively. Categorical data are presented as counts and compared using Fisher's exact test.

<sup>a</sup>Aspirin (n = 1), clopidogrel (n = 1), aspirin + clopidogrel (n = 1).

<sup>b</sup>Aspirin (n = 2).

<sup>c</sup>qSOFA = quick sequential organ failure assessment score.

<sup>d</sup>MEWS = modified early warning score.

<sup>e</sup>PSI = pneumonia severity index.

<sup>f</sup>Measured upon presentation to the emergency department (for patients).

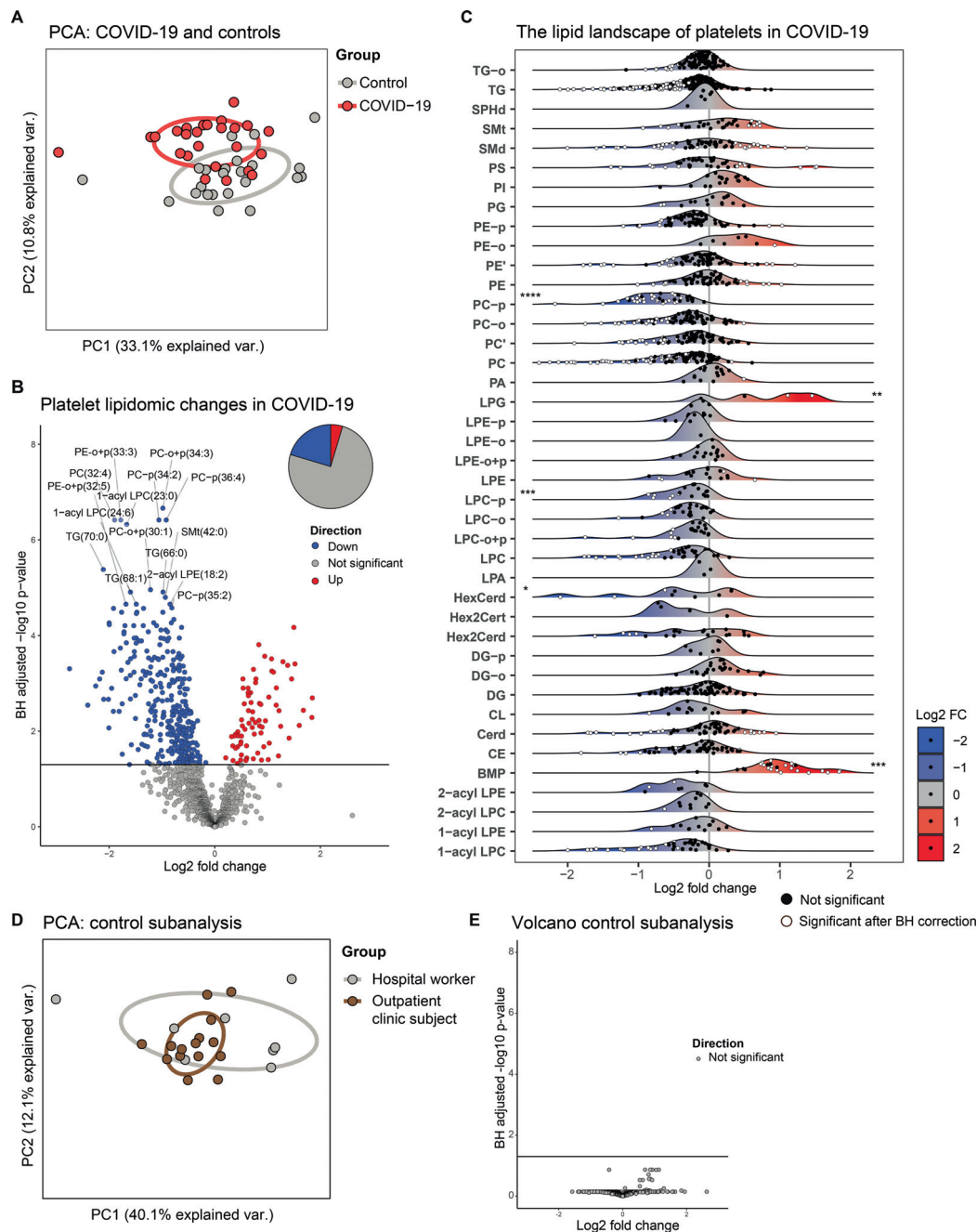


**Fig. 1** The platelet lipidome is altered in patients with COVID-19. (A) Principal component analysis (PCA) of the platelet lipidomes, comprising all lipids normalized on specific internal standards per class, of patients with COVID-19 ( $n = 25$ ) and matched controls ( $n = 23$ ). Each dot represents a subject, the color represents the group. X-axis shows the first principal component and the percentage of explained variance, the Y-axis shows the second principal component and the percentage of explained variance. (B) Volcano plot showing the differential abundance of lipids in platelets from patients with COVID-19 and matched controls. Each dot represents a lipid species, while the color indicates whether the lipid is significantly more abundant (red), significantly less abundant (blue), or not significantly altered (gray). The X-axis denotes the log<sub>2</sub> fold change between groups, while the Y-axis shows the Benjamini–Hochberg adjusted  $-\log_{10} p$ -value. The pie chart represents the whole platelet lipidome and gives an indication of the percentage of lipids that is either more abundant, less abundant, or unchanged. (C) Platelet lipid landscape plots, comparing patients with COVID-19 to matched controls. Each dot represents a lipid species, which are grouped per lipid class. The color of the dots indicates whether the lipid was significantly different (white) or not (black) between the groups after Benjamini–Hochberg correction. The X-axis shows the log<sub>2</sub> fold change between groups for each lipid; the color of the ridges indicates up- (red) or down-regulated (blue) lipids. The Y-axis indicates the different lipid classes, with a ridge plot per lipid class that shows the distribution of the lipids within their respective classes. On the edges of the plot, asterisks denote class-wide significant differences as determined by a Wilcoxon-ranked sum test of aggregated values per class (a sum of all lipids per class per subject). Asterisks on the left of the plot indicate a significant class-wide decrease, and asterisks on the right of the plot indicate a significant class-wide increase. A  $p$ -value below 0.05 was considered significant. (D) Same as in panel (A), but here showing the control sub-analysis (hospital workers vs. outpatient clinic subject). (E) Same as in panel (B), but here showing the control sub-analysis (hospital workers vs. outpatient clinic subject). \* $p$ -value < 0.05, \*\* $p$ -value < 0.01, \*\*\* $p$ -value < 0.001, \*\*\*\* $p$ -value < 0.0001. All boxplots of this analysis are shown in ► **Supplementary Fig. S2**.



between the groups. Interestingly, the significantly altered part of the platelet lipidome mostly comprised lipids that were less abundant in patients with COVID-19 (20.4% down, 4.6% up, 75% unchanged). The top 15 differentially abundant lipids (all downregulated in platelets from COVID-19 patients relative to controls) mainly included species belonging to (lyso)phospholipid classes, which have both structural and signaling roles.

While data on single lipid species can be very insightful in the context of lipid signaling, a uniform shift of a related group of lipids may offer extra biological information. To illustrate the direction, distribution, and significance of change for each lipid within a class, we constructed a ridge plot for each lipid class (►Fig. 1C). All class-wide comparisons are shown in ►Fig. S1. This analysis revealed three main findings, upon which we expand in the next paragraphs<sup>1</sup>: class-wide lower abundances of phosphatidylcholine plasmalogen (PC-p) and lysophosphatidylcholine plasmalogen (LPC-p) lipids in platelets from COVID-19 patients relative to controls,<sup>2</sup> class-wide higher abundances of lysophosphatidylglycerol (LPG) and bis(monoacylglycerol) phosphate (BMP) in patients' platelets,<sup>3</sup> a specific group of decreased triacylglycerol lipids in patients with COVID-19 (►Fig. 1C). Of note, subgroup analysis within the control group—health care workers and outpatient clinic patients—did not show significant differences (►Fig. 1D, E).

### A Decrease of Plasmalogens in Platelets of Patients with COVID-19

Plasmalogens (PC-p, PE-p, LPC-p, LPE-p) are a subclass of peroxisome-derived glycerophospholipids characterized by their vinyl-ether bond on the *sn*-1 position of the glycerol backbone, whereas other more common glycerophospholipids contain ester bonds.<sup>19</sup> Diverse cellular functions, such as membrane fusion and lipid raft signaling, are enabled in part by this simple biochemical modification. Strikingly, we observed a specific decrease of PC-p lipids in platelets from patients with COVID-19, while other PC subclasses—not containing a vinyl-ether bond—did not show class-wide changes (►Figs. 1C and 2A). PC lipids are the main constituents of the outer cell membrane, and the composition and saturation of PC regulate cell membrane fluidity, surface protein interactions, and membrane fusion.<sup>11</sup> The specific decrease of PC plasmalogens was corroborated by the observation of a similar pattern for the LPC-p class (►Fig. 2A), which is mainly generated by enzymatic hydrolysis of PC via cytoplasmic phospholipase A2 (cPLA2) activity.<sup>20</sup>

### Increase of Platelet LPG and BMP in COVID-19, Correlation with Platelet Reactivity

The lipid classes LPG and BMP were significantly increased in patients with COVID-19 (►Figs. 1C and 2B). These classes are intimately related: phosphatidylglycerol (PG), via LPG, is a precursor of BMP, which is a structural isomer of PG.<sup>21</sup> LPG is thought to activate G-protein-coupled receptors, resulting in downstream calcium mobilization in other cell types.<sup>20</sup> BMP is almost exclusively present in late endosomes or lysosomes, and closely involved in vesicular trafficking.<sup>22</sup> Others and we

previously showed that platelets from COVID-19 patients have an increased reactivity to thrombin receptor PAR1 stimulation (shown for the population reported here in ►Fig. 2C).<sup>4,5,8</sup> Given the observed increase of LPG and BMP in resting platelets from patients with COVID-19, and their presumed role in intracellular calcium signaling and granule trafficking, we next investigated if the abundance of these lipid classes was linked to platelet reactivity to thrombin. LPG levels—and to a lesser extent BMP levels—were strongly correlated to platelet reactivity to thrombin, as evaluated by P-selectin expression upon PAR1 stimulation (►Fig. 2D). This association was present both in COVID-19 patients and controls, suggesting a fundamental link between platelet LPG/BMP levels and platelet reactivity to thrombin (►Fig. 2E).

### Decrease of Long-Chain, Highly Saturated Triacylglycerol

While triacylglycerol (TG) species did not show a class-wide difference (►Fig. 3A), a substantial subset of TGs was significantly decreased in platelets from patients with COVID-19 (►Fig. 1C). To investigate what distinguished decreased TG from unaltered platelet TG, we studied the length and the level of unsaturation (number of double bonds) for TG species and visualized the fold change between patients and controls (►Fig. 3B). Specifically, long-chain, highly saturated TG species (defined as 60–72 carbons long and 0–6 double bonds), were significantly less abundant in platelets from patients with COVID-19.

## Discussion

While a few studies recently laid the groundwork for the field of platelet lipidomics, the lipidome of human platelets during a state of infection thus far has remained unexplored.<sup>14,15,23</sup> Here, we present an untargeted analysis of the lipidome of platelets in patients with COVID-19 and noninfectious controls.

Twenty-five percent of the platelet lipidome was significantly different between patients with COVID-19 and controls. Two of the major platelet lipidomic studies published thus far reported perturbation of a similar proportion of the platelet lipidome of healthy subjects after ex vivo stimulation.<sup>14,23</sup> Thus, while lipidome metabolism and remodeling might be crucial for platelet activity,<sup>24</sup> the majority of the lipidome appears to remain stable throughout ex vivo activation and in COVID-19. This may indicate that most of the platelet lipidome sustains integral cellular processes and structures—such as the plasma membrane and intracellular organelles. Interestingly, while the majority of earlier reports focused on upregulated lipid species, most of the significantly altered lipids in our study were decreased in platelets from patients with COVID-19. Overall, it remains uncertain how the lipidomic findings of ex vivo stimulated platelets<sup>14,23</sup> translate to the biological state of platelets during disease such as in our study. While platelets in COVID-19 are activated,<sup>8</sup> this activation is most likely more subtle and multifactorial than after direct ex vivo stimulation.

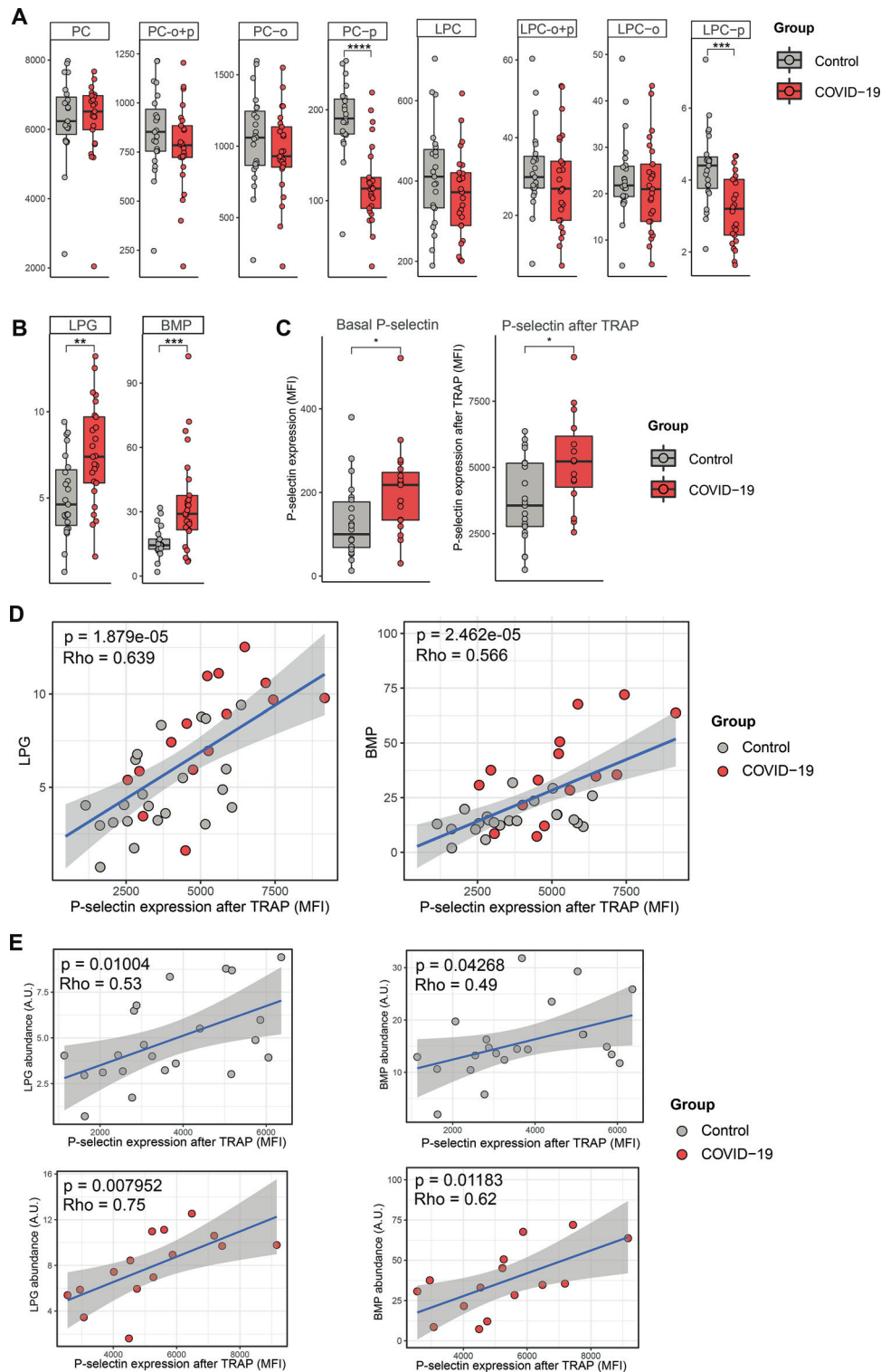


**Fig. 2** Class-wide lipidomic changes in COVID-19 and correlation with platelet reactivity. (A) Boxplots showing the median and interquartile ranges of PC and LPC subclasses. Each point shows the aggregated values per lipid class (a sum of all lipids per class) per subject, thus each point represents an individual. Values on the y-axis are semiquantitative lipid abundance (arbitrary unit, A.U). A  $p$ -value below 0.05 was considered significant after a Wilcoxon-ranked sum test. (B) Boxplots of LPG and BMP lipid classes. (C) Boxplots showing P-selectin expression (in MFI) on platelets in the basal state or after stimulation with TRAP, comparing patients with COVID-19 and matched controls. For both boxplots, a  $p$ -value below 0.05 was considered significant after a Wilcoxon-ranked sum test. \* $p$ -value < 0.05. (D) Scatterplots showing the correlation between aggregated LPG (left) and BMP (right) levels and platelet P-selectin expression (in MFI) after stimulation with TRAP. Values on the y-axis are semiquantitative lipid abundances (arbitrary unit, A.U). The strength of the correlation is depicted as Spearman's rho. (E) Same as in panel (D), but now split between controls and patients. BMP, bis(monoacylglycerol)phosphate; LPC, lysophosphatidylcholine; LPG, lysophosphatidylglycerol; MFI, median fluorescence intensity; PC, phosphatidylcholine.

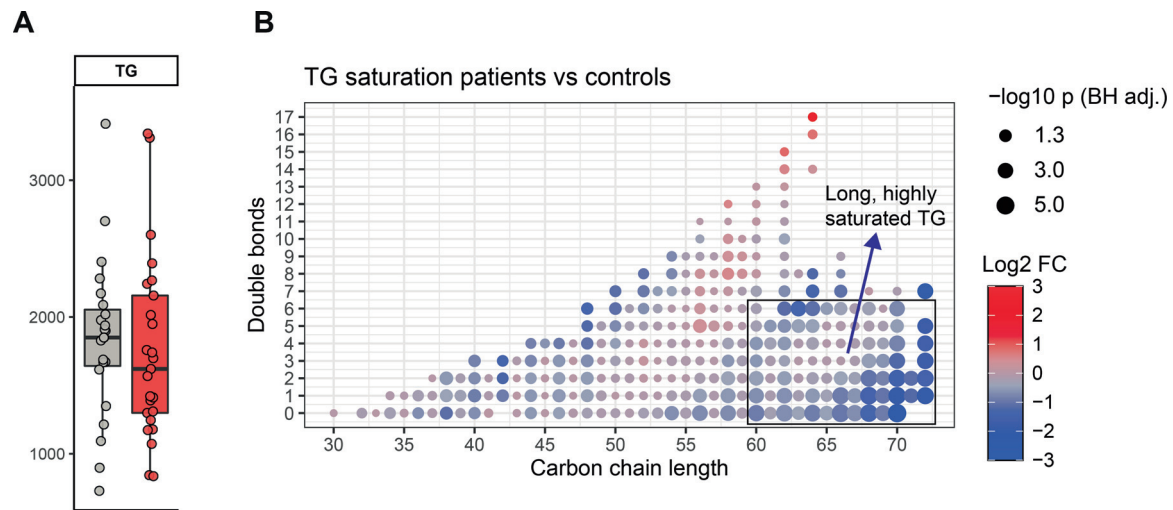


**Fig. 3** Decrease of long-chain, highly saturated triacylglycerol in COVID-19 platelets. (A) Boxplot of the TG class. (B) Dot plot of TG differences between patients with COVID-19 and controls. Each dot is a TG species. The color of the dots indicates the log<sub>2</sub>-fold change between the groups, the size of the dot is proportional to the Benjamini–Hochberg adjusted  $-\log_{10} p$ -value of this change. The X-axis indicates the carbon chain length, and the Y-axis shows the amount of double bonds in the lipid.

The decrease of plasmalogen membrane lipids (PC-p) in platelets from patients with COVID-19 is striking. Plasmalogens are a subclass of lipids that are characterized by a vinyl-ether bond, which provides several distinct functions.<sup>19</sup> Cellular plasmalogen loss was observed in other pathological conditions such as neurodegenerative and metabolic diseases, two conditions where oxidative stress is presumed to play an important pathophysiological role.<sup>19,25</sup> While further research is necessary to reveal the mechanisms by which plasmalogens could participate in disease pathophysiology, part of the explanation could lie within their potential role as reactive oxygen species scavengers.<sup>26</sup> As plasmalogens are preferentially oxidized over the double bonds in other unsaturated membrane lipids, they can function as a shield against free radicals: decreased plasmalogen levels may be the result of high oxidative stress. Additionally, PC-p is an important source of fatty acids, which in turn are substrates for  $\beta$ -oxidation but also potent proinflammatory lipid mediators.<sup>27</sup>

While plasmalogens were less abundant in platelets from patients with COVID-19, we observed a clear class-wide increase of both BMP and its biosynthetic precursor LPG. Importantly, LPG and BMP both strongly correlated with platelet reactivity to PAR1 activation, irrespective of disease state. It could be hypothesized that LPG and BMP synthesis is increased upon activation, and that the higher LPG and BMP levels in patients with COVID-19 are reflective of their increased platelet activation status. BMPs are exclusively localized in late endosomes and lysosomes in cells, and most reports describe an integral role of BMP in endosomal trafficking.<sup>22</sup> The increased amounts of BMP in platelets from patients with COVID-19 could be indicative of higher dense granule content—a lysosome-related organelle essential for platelet activation.<sup>28</sup>

We observed that the impact of COVID-19 on triacylglycerols was at least in part dependent on the saturation and

length of the lipids. The cause and potential functional consequences of this decrease in specific TG subsets remain speculative. Platelets use  $\beta$ -oxidation of fatty acids upon activation to provide energy for cellular structural changes.<sup>23,29</sup> As very long-chain fatty acids and medium-chain fatty acids undergo different metabolic processing because of enzyme selectivity in fatty-acid oxidation,<sup>30</sup> the observed difference might indicate a change in fatty-acid metabolism.

While it would be interesting to compare our results with findings in other patient groups, the platelet lipidome is yet to be explored in most disease states. The field of atherothrombosis is an exception. In a targeted analysis, Chatterjee et al reported an increase of nonenzymatically oxidized lipids, ceramides, di- and triacylglycerol, and sphingomyelin lipids in platelets of patients with symptomatic coronary artery disease.<sup>31</sup> Another, recent investigation performed untargeted platelet lipidomics in 139 patients with chronic or acute coronary syndrome, identifying a relatively small proportion of significantly different lipids.<sup>15</sup> Interestingly, alkenyl or alkylether linkage was one of the common characteristics of the upregulated PCs. The authors also reported a decreased amount of some TG, PCs, and sphingomyelin species in coronary artery disease patients, with a correlation with disease stability. These pioneering studies show an opposed directional effect when compared with our findings in patients with COVID-19, in whom most platelet lipid classes—and specifically PC-p—were less abundant when compared with controls. Together, it appears that the lipidomic perturbation of platelets during infection is relatively large compared with other prothrombotic states, and that different lipid classes are differentially regulated between these conditions.

Our study has several limitations. First, the studied sample size is relatively limited, as using clinical samples for such



extensive analytical pipelines is challenging. Second, although we maintained a strict inclusion window, and specifically focused on patients on the ward, some heterogeneity invariably exists within the patient group. It is possible that the platelet lipidome is influenced by the time since onset of symptoms, as well as other variation in baseline characteristics. We did not have the opportunity to include patients with other infections as controls, so whether the observed changes are pathogen-specific remains to be elucidated. Finally, we were not able to implement lipidomic interventions in these samples, so future mechanistic studies are needed to confirm the observed correlations between the lipidome and platelet reactivity.

In conclusion, we report distinctive lipidomic changes in platelets from patients with COVID-19 when compared with noninfectious controls. These results provide the first indication of the profound impact of infection on the human platelet lipidome. This warrants further investigation in other infections and disease states that involve platelet pathophysiology, with an emphasis on the functional implications of lipidomic perturbations.

### What is known about this topic?

- Platelets are hyperactivated in patients with COVID-19.
- The lipidome of platelets has been shown to be important for platelet functionality and activation in controlled settings.
- The lipidome of platelets during infection has remained unexplored thus far.

### What does this paper add?

- Twenty-five percent of the lipidome of platelets is altered in patients with COVID-19.
- Platelets from COVID-19 patients showed decreased levels of membrane plasmalogens, and a distinct decrease of long-chain, unsaturated triacylglycerols.
- The lipid classes LPG and BMP are increased in patients with COVID-19, and levels correlate to platelet reactivity to thrombin, irrespective of disease state.

### Data Sharing Statement

The data that support the findings of this study are available from the corresponding author.

### Funding

This work was supported by the Netherlands Organization for Health Research and Development (ZonMW grant #50-53000-98-139 to T.v.d.P.). V.L. is supported by Assistance Publique des Hôpitaux de Paris, Fondation Bettencourt-Schueller; L.P. is supported by JPI-AMR/ZonMW #547001008; O.C. is supported by Landsteiner Foundation (LSBR # 1901). T.D.Y.R. is supported by NACTAR (# 16447) financed by the Dutch Research Council (NWO). The

fundors had no role in study design, data collection and analysis, decision to publish, or preparation of the manuscript.

### Conflict of Interest

None declared.

### References

- 1 Helms J, Tacquard C, Severac F, et al; CRICS TRIGGERSEP Group (Clinical Research in Intensive Care and Sepsis Trial Group for Global Evaluation and Research in Sepsis) High risk of thrombosis in patients with severe SARS-CoV-2 infection: a multicenter prospective cohort study. *Intensive Care Med* 2020;46(06):1089–1098
- 2 Leentjens J, van Haaps TF, Wessels PF, Schutgens REG, Middeldorp S. COVID-19-associated coagulopathy and antithrombotic agents—lessons after 1 year. *Lancet Haematol* 2021;8(07):e524–e533
- 3 Middeldorp S, Coppens M, van Haaps TF, et al. Incidence of venous thromboembolism in hospitalized patients with COVID-19. *J Thromb Haemost* 2020;18(08):1995–2002
- 4 Manne BK, Denorme F, Middleton EA, et al. Platelet gene expression and function in patients with COVID-19. *Blood* 2020;136(11):1317–1329
- 5 Zhang S, Liu Y, Wang X, et al. SARS-CoV-2 binds platelet ACE2 to enhance thrombosis in COVID-19. *J Hematol Oncol* 2020;13(01):120
- 6 Bury L, Camilloni B, Castronari R, et al. Search for SARS-CoV-2 RNA in platelets from COVID-19 patients. *Platelets* 2021;32(02):284–287
- 7 Zaid Y, Puhm F, Allaey S, et al. Platelets can associate with SARS-CoV-2 RNA and are hyperactivated in COVID-19. *Circ Res* 2020;127:1404–1418
- 8 Léopold V, Pereverzeva L, Schuurman AR, et al. Platelets are hyperactivated but show reduced glycoprotein VI reactivity in COVID-19 patients. *Thromb Haemost* 2021;121(09):1258–1262
- 9 Nicolai L, Leunig A, Brambs S, et al. Immunothrombotic dysregulation in COVID-19 pneumonia is associated with respiratory failure and coagulopathy. *Circulation* 2020;142(12):1176–1189
- 10 Taus F, Salvagno G, Canè S, et al. Platelets promote thromboinflammation in SARS-CoV-2 pneumonia. *Arterioscler Thromb Vasc Biol* 2020;40(12):2975–2989
- 11 O'Donnell VB, Murphy RC, Watson SP. Platelet lipidomics: modern day perspective on lipid discovery and characterization in platelets. *Circ Res* 2014;114(07):1185–1203
- 12 McMahon HT, Boucrot E. Membrane curvature at a glance. *J Cell Sci* 2015;128(06):1065–1070
- 13 Bodin S, Tronchère H, Payrastre B. Lipid rafts are critical membrane domains in blood platelet activation processes. *Biochim Biophys Acta* 2003;1610(02):247–257
- 14 Peng B, Geue S, Coman C, et al. Identification of key lipids critical for platelet activation by comprehensive analysis of the platelet lipidome. *Blood* 2018;132(05):e1–e12
- 15 Harm T, Bild A, Dittrich K, et al. Acute coronary syndrome is associated with a substantial change in the platelet lipidome. *Cardiovasc Res*. Doi: 10.1093/cvr/cvab238
- 16 Haak BW, Brands X, Davids M, et al. Bacterial and viral respiratory tract microbiota and host characteristics in adults with lower respiratory tract infections: a case-control study. *Clin Infect Dis* 2022;74(05):776–784
- 17 Molenaars M, Schomakers BV, Elfrink HL, et al. Metabolomics and lipidomics in *Caenorhabditis elegans* using a single-sample preparation. *Dis Model Mech* 2021;14(04):dmm047746
- 18 Jolliffe IT, Cadima J. Principal component analysis: a review and recent developments. *Philos Trans- Royal Soc, Math Phys Eng Sci* 2016;374(2065):20150202

- 19 Dean JM, Lodhi IJ. Structural and functional roles of ether lipids. *Protein Cell* 2018;9(02):196–206
- 20 Grzelczyk A, Gendaszewska-Darmach E. Novel bioactive glycerol-based lysophospholipids: new data – new insight into their function. *Biochimie* 2013;95(04):667–679
- 21 Bouvier J, Zemski Berry KA, Hullin-Matsuda F, et al. Selective decrease of bis(monoacylglycero)phosphate content in macrophages by high supplementation with docosahexaenoic acid. *J Lipid Res* 2009;50(02):243–255
- 22 Showalter MR, Berg AL, Nagourney A, Heil H, Carraway KL III, Fiehn O. The emerging and diverse roles of bis(monoacylglycero) phosphate lipids in cellular physiology and disease. *Int J Mol Sci* 2020;21(21):8067
- 23 Slatter DA, Aldrovandi M, O'Connor A, et al. Mapping the human platelet lipidome reveals cytosolic phospholipase A2 as a regulator of mitochondrial bioenergetics during activation. *Cell Metab* 2016;23(05):930–944
- 24 Lepropre S, Kautbally S, Octave M, et al. AMPK-ACC signaling modulates platelet phospholipids and potentiates thrombus formation. *Blood* 2018;132(11):1180–1192
- 25 Wood PL, Locke VA, Herling P, et al. Targeted lipidomics distinguishes patient subgroups in mild cognitive impairment (MCI) and late onset Alzheimer's disease (LOAD). *BBA Clin* 2015; 5:25–28
- 26 Broniec A, Klosinski R, Pawlak A, Wrona-Krol M, Thompson D, Sarna T. Interactions of plasmalogens and their diacyl analogs with singlet oxygen in selected model systems. *Free Radic Biol Med* 2011;50(07):892–898
- 27 Dalli J, Colas RA, Quintana C, et al. Human sepsis eicosanoid and proresolving lipid mediator temporal profiles: correlations with survival and clinical outcomes. *Crit Care Med* 2017;45(01):58–68
- 28 Ambrosio AL, Di Pietro SM. Storage pool diseases illuminate platelet dense granule biogenesis. *Platelets* 2017;28(02):138–146
- 29 Ravi S, Chacko B, Sawada H, et al. Metabolic plasticity in resting and thrombin activated platelets. *PLoS One* 2015;10(04):e0123597
- 30 Han X. Lipidomics for studying metabolism. *Nat Rev Endocrinol* 2016;12(11):668–679
- 31 Chatterjee M, Rath D, Schlotterbeck J, et al. Regulation of oxidized platelet lipidome: implications for coronary artery disease. *Eur Heart J* 2017;38(25):1993–2005